Proceedings 18th NZ Geothermal Workshop 1996

NUMERICAL SIMULATION OF SILICA SCALING

J. POTT[1,2], M.G. DUNSTALL[2], K.L. BROWN[2,3]

[1] University of Stuttgart, Germany
[2] Geothermal Institute, The University of Auckland, NZ
[3] Wairakei Research Centre, IGNS, Taupo, NZ

SUMMARY - The scaling of silica colloids on the surface of a flat plate is numerically simulated using the software package PHOENICS. Emphasis is put on providing a link between the fluid flow and the scaling process. Formulations for the mechanisms leading to the deposition of silica are derived and the appropriate computer coding is added to PHOENICS. The influence of colloid size is investigated and the simulations predict the initial distribution of silica scale on the plate.

1. INTRODUCTION

Geothermal fluids contain considerable quantities of dissolved solids of which silica in particular can cause severe scaling problems. The formation of silica scale in pipelines, heat exchangers, and reinjection wells is a limiting factor in the utilisation of high temperature geothermal resources. Therefore, a reduction of the scaling rate results in more efficient use of geothermal energy.

The influence of fluid chemistry and temperature on the process of silica scaling is well established. However, little research has been performed in order to investigate hydrodynamic effects on scaling. Therefore, the task of this project is the numerical simulation of silica deposition as a function of fluid flow.

The computational fluid dynamics software package PHOENICS was chosen for the simulation of the flow of the geothermal fluid which is assumed to be supersaturated with colloidal silica. Additional coding was developed to take account of the mechanisms that promote colloid movement towards a surface and hence lead to scaling. Two-dimensional simulations were conducted for the hydrodynamically well examined and prescribed geometry of a flat plate in parallel laminar flow.

2. NUMERICAL MODELLING

PHOENICS is a computer code for the numerical simulation of single and multi-phase flow, heat and mass-transfer, and various chemical reaction phenomena. One of the major advantages of the package is the possibility for the user to extend its performance by supplementing the existing computer coding. PHOENICS is based on the finite volume method. Therefore, the solution domain is subdivided into a set of control volumina. Application of the law of conservation to single control volumina leads to the discretised versions of the governing differential equations. The equations of fluid motion for the continuous phase are solved within the main module of PHOENICS and a particle tracking subroutine GENTRA takes account of the motion of the silica colloids.

The simulations were performed on an IBM RISC System/6000 using the PHOENICS version 2.1.3.

2.1 Representation of the continuous phase

The equations governing the motion of a fluid are derived from the conservation laws for mass and momentum. Applying conservation of mass leads to the continuity equation. For an incompressible fluid the equation of continuity assumes the form:

$$\nabla \cdot \mathbf{v} = 0 \qquad (1)$$

where **v** denotes the velocity vector. Conservation of momentum leads to the Navier-Stokes equations which, for incompressible viscous flow, can be presented as:

$$\rho\left(\frac{\partial \mathbf{v}}{\partial t} + \mathbf{v} \cdot \nabla \mathbf{v}\right) = \mathrm{F} - \nabla p + \mu \nabla^2 \mathbf{v} \qquad (2)$$

where F expresses body forces per unit volume and p denotes the pressure. ρ and μ are the density and dynamic viscosity of the fluid, respectively.

The continuity equation of mass and the Navier-Stokes equations provide four equations for the full description of three-dimensional viscous fluid flow, which is characterised by the pressure and the three components of velocity.

2.2 Representation of the particulate phase

The subroutine GENTRA solves the particle equations and provides detailed information on the particle behaviour in form of trajectories. The approach is based on the Particle-Source-In-Cell method of Crowe **(1977).** The subscripts c and p describe the continuous and particulate phase, respectively.

The particle momentum equation - The velocity of the particle v, is computed from the particle momentum equation:

$$m_P \frac{dv_P}{dt} = D_P(v_C - v_P) + m_P\left(1 - \frac{\rho_C}{\rho_P}\right)g - V_P \nabla p \quad (3)$$

The first term on the right-hand side of equation (3) represents the drag force exerted on the particle by the continuous phase. The second and third terms represent the gravitational force and a pressure gradient related source of momentum. The velocity components of the continuous phase v, are interpolated at the particle position from the values of the neighbouring volumina.

The particle position equation - The particle position x_P is determined by integration of the following equation:

$$\frac{dx_P}{dt} = v_P \quad (4)$$

2.3 Representation of additional influences

The integration of the particle equations leads to the particle trajectories. Only one particle is tracked at a time and therefore particle to particle interactions such as concentration effects are not considered. However, GENTRA provides the opportunity to alter the particle equations and hence to supplement the performance of the particle tracking. The user accessible area of GENTRA is called at well defined stages during the solution procedure of the particulate phase equations.

2.4 The solution procedure

GENTRA is called by PHOENICS between iteration sweeps of the computational domain, which PHOENICS performs to solve the continuous phase equations. GENTRA then tracks the particles as they move through the computed flow field, calculating in the process the transfer of momentum between the two phases. After leaving GENTRA, these interface interactions are incorporated as source terms in the continuous phase equations for the next PHOENICS sweep.

3. SILICA SCALING

During exploitation of a geothermal field hot fluid is brought to the surface where its thermal energy is utilised. As a result of steam extraction or heat transfer the likelihood of precipitation of dissolved solids increases. In particular amorphous silica is formed at concentrations high enough to cause serious scaling. In fluids supersaturated with respect to amorphous silica the mechanism responsible for the majority of silica deposition is the preliminary formation of colloids and their subsequent precipitation. Only colloidal deposition is investigated in the following and scaling by monomeric silicic acid is neglected. The term silica concentration therefore implies colloidal silica concentration.

A colloidal system consists of small particles of one substance distributed throughout the continuous phase of another substance. As a result of their small dimensions, colloids are subject to Brownian motion. The large negative surface charge together with the Brownian motion of silica colloids enable their suspension in solution and maintain the stability of the colloidal system.

3.1 Deposition of silica colloids

In the following several different mechanisms responsible for the precipitation of silica colloids are discussed.

Flocculation of colloids - Flocculation is a process where colloids combine and precipitate out of solution due to their increased molecular weight. The fusion of colloids can be triggered by two different processes. The surfaces of the silica colloids are negatively charged and cations in solution act as bridges between neighbouring colloids. However, flocculation through bridging is restricted to very small particles, i.e. radii of a few nm. The second possibility for two colloids to merge results from the high degree of supersaturation. As a result of Brownian motion the colloids get close enough to overcome the electrostatic repulsion and aggregate. For the modelling of the colloidal system it can be assumed that the diameter and the surface charge of the silica particles is large enough to prevent the fusion of colloids and their subsequent deposition.

Electrostatic forces - Ionisation of surface-OH groups results in silica colloids having a large negative surface charge. For the preliminary process of scaling, electrostatic forces between the charged colloids and the neutral surface of a wall are assumed to be negligible. During further build-up of scale the upper surface of silica scale will be negatively charged, and electrostatic repulsion forces might decrease the rate of colloid deposition. As will be discussed later, the current attempt to model silica deposition assumes validity only for the initial process of scaling and electrostatic effects are therefore negligible.

The concentration force - The mechanism assuming major importance for the scaling of silica colloids results from local variations of the silica concentration near a surface. It can be described in terms of a fictitious force acting on a colloid. According to the molecular kinetic theory silica colloids are subject to Brownian motion. This random motion is the origin of the diffusion of particles under the concentration gradient $\partial C/\partial y$, and the particle flux J can be expressed by Fick's first law of diffusion:

$$J = -D_C \frac{\partial C}{\partial y} \quad (5)$$

D, is called the diffusion coefficient and is determined by the Stokes-Einstein relation:

$$D_C = \frac{kT}{f} \quad ; \qquad f = 3\pi\nu\rho d_P \quad (6)$$

where T is the temperature and k the Boltzmann constant. For spherical particles of diameter d, the friction coefficient f is given by Stokes' law. ρ and v denote the fluid density and kinematic viscosity, respectively. The process of diffusion can also be described in terms of a fictitious force acting on the particles in the direction of the concentration gradient. According to van de Ven **(1989)** the concentration force for a single particle assumes the form:

$$F_C = -\frac{kT}{C}\frac{\partial C}{\partial y} \quad (7)$$

So far, no formulation expressing the concentration **C** as a function of coordinates x, y relative to the surface has been derived. This concentration equation will be determined in section 4 by introducing the boundary-layer concept.

3.2 Addition of the concentration force

Since concentration effects are not considered by **GENTRA** the concentration force (7) is calculated at every particle position and its value is added to the momentum equation for the particulate phase (3). This is achieved by inserting the appropriate coding in the user accessible subroutine of **GENTRA.**

3.3 Representation of the colloidal system

The numerical simulation of the process of silica scaling requires various assumptions. The colloidal system is regarded as being stable. The colloids are assumed to be of spherical shape and, during each simulation, are of constant uniform diameter. Measurements on silica colloids in the Wairakei geothermal area determined typical values for the colloid diameter d, and the mass concentration C, of the colloidal system as shown in Table 1. The value of the colloid density ρ_P lies between the densities of quartz and water and was estimated to 1500kg/m³. For T = 20°C the values for the diffusion coefficient D„ the particle mass m_P, and the silica concentration, later referred to as the free-stream concentration C_∞, are calculated.

Table 1- Properties of the colloidal system for T=20°C

measured values:	d, = 50 nm
	C, = 500 mg/kg
estimated value:	ρ_P = 1500 kg/m³
calculated values:	D, = **8.585E-12** m²/s
	m_P = **9.818E-20** kg
	C_∞ = **5.093E09** particles/mm³
(for ρ = 1000 kg/m³ and v = **1.0E-06** m²/s)	

Once a silica colloid gets within very short range of a surface the van de Waals attraction forces enable the colloid to adhere to the surface. To a small extent, amorphous silica might redissolve in solution but this effect can be excluded for entire colloids. The plate acts as a sink for colloids, and therefore the concentration at the surface equals zero.

4. CONVECTIVE MASS TRANSFER

In the following, a formulation for the distribution of silica colloids near a surface is derived. The convective transfer of colloids between the free-stream fluid and the plate depends on the properties of the fluid and the colloids, surface geometry, and flow conditions. Appropriate equations are obtained by introducing the concept of boundary layers for laminar flow over a flat plate at zero incidence angle.

4.1 The velocity boundary layer

A viscous fluid adheres to the plate surface and frictional forces retard the motion of the fluid in the adjoining fluid layers. The distance from the plate at which the frictional forces become negligible is called the velocity-boundary-layer thickness δ. It is defined as the value of y for which the velocity component in the x-direction u assumes **99%** of the free-stream velocity u_∞. Figure 1 shows the velocity distribution in the velocity boundary layer with the dimensions across it considerably exaggerated.

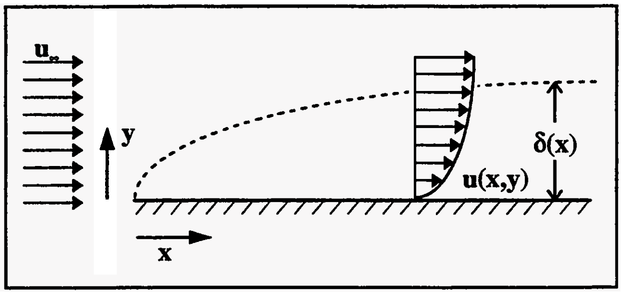

Figure 1 - Velocity boundary layer for laminar flow

For the description of the fluid flow within the boundary layer the velocity profile must be derived. Assuming that the velocity varies as a power series across the boundary layer it can be represented as:

$$u = a_0 + a_1 y + a_2 y^2 + a_3 y^3 \quad (8)$$

where y is the distance perpendicular to the plate and a_{0-3} are constants. The equation is subject to four boundary conditions:

$$u\big|_{y=0} = 0 \qquad \text{(adhesion at the plate)}$$

$$\left.\frac{\partial^2 u}{\partial y^2}\right|_{y=0} = 0 \qquad \text{(constant surface shear stress)}$$

$$u\big|_{y=\delta} = u_\infty \qquad \text{(outside the boundary layer the}$$

$$\left.\frac{\partial u}{\partial y}\right|_{y=\delta} = 0 \qquad \text{flow is not influenced by plate)}$$

With these boundary conditions the constants in equation **(8)** can be found and the velocity profile within the boundary layer is given by:

$$u = 1.5\frac{u_\infty}{\delta}y - 0.5\frac{u_\infty}{\delta^3}y^3 \qquad (9)$$

A formulation for the velocity-boundary-layer thickness 6 can be determined by applying mass and momentum balances in combination with the surface shear stress, as shown by Cussler **(1984):**

$$\delta = \left(\frac{280}{13}\right)^{0.5}\left(\frac{\nu\, x}{u_\infty}\right)^{0.5} \approx 4.64\sqrt{\frac{\nu\, x}{u_\infty}} \qquad (10)$$

With increasing distance x from the leading edge of the plate the velocity boundary layer grows continuously. The foregoing calculation is approximate, subject to a variety of assumptions. To verify the quality of the derived velocity profile, the results of applying equations **(9)** and **(10)** are compared to the exact solution of the Navier-Stokes equations within the velocity boundary layer, which are described by Schlichting **(1979).** Figure **2** shows the good agreement between the approximate and the exact solutions.

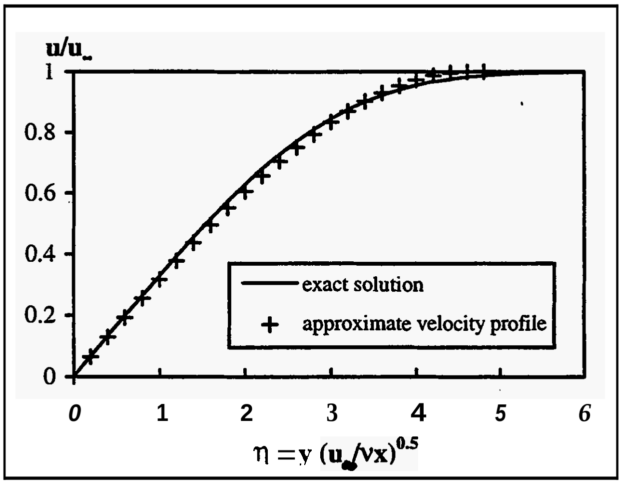

Figure 2 - Dimensionless velocity profile

4.2 The concentration boundary layer

A concentration boundary layer also develops on the surface of the plate, similar to the velocity boundary layer. Within the concentration boundary layer the colloids are transported by advection with the mean velocity of the fluid and by diffusion relative to the bulk motion. Assuming that the concentration C can be expressed as a power series, and applying boundary conditions as before, leads to the equation for the concentration profile within the concentration boundary layer:

$$C = 1.5\frac{C_\infty}{\delta_C}y - 0.5\frac{C_\infty}{\delta_C^3}y^3 \qquad (11)$$

where C_∞ denotes the free-stream concentration. The thickness of the concentration boundary layer δ_C can be derived through application of a mass balance in combination with Fick's law of diffusion:

$$\delta_C = \left(\frac{280}{13}\right)^{0.5}\left(\frac{\nu\, x}{u_\infty}\right)^{0.5}\left(\frac{D_C}{\nu}\right)^{0.33} = \delta\, Sc^{-0.33} \qquad (12)$$

The Schmidt number Sc denotes the ratio of momentum and mass diffusivities. Equation **(12)** shows that the concentration-boundary-layer thickness is proportional to the velocity-boundary-layer thickness.

With the formulation for the concentration **(11)** all components of equation (7), representing the concentration force F_C acting on a particle within the concentration boundary layer, are determined and the force can be added to the momentum equation **(3).**

5. RESULTS

The parameter that is varied in the simulations presented in this section is the particle diameter d,. The temperature, as well as properties of the colloids, the colloidal system, and the fluid are not subject to changes and assume the values assigned in section **3.3.** The free-stream velocity is **3m/s.** Figure **3** shows the boundary-layer development. The concentration boundary layer δ_C, given for a particle diameter of 50nm, is about fifty times smaller than the velocity boundary layer 6.

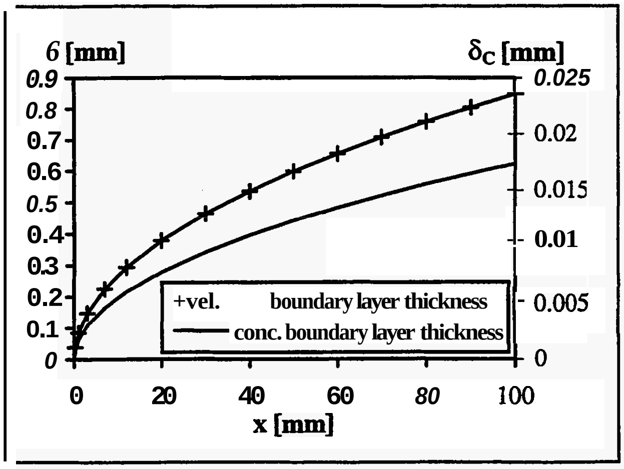

Figure 3 - Development of the velocity and concentration boundary layers

For the derivation of the concentration profile **(11)** diffusion in the x-direction was assumed to be negligible. As can be seen in Figure **3,** the gradient of the concentration-boundary-layer thickness at the leading edge of the plate, x = 0, is infinite and therefore considerable diffusion in the x-direction is expected. However, the gradient decreases rapidly along the plate and the derived equations assume validity after approximately 1ym. With increasing distance from the leading edge the flow within the boundary layer changes from a highly ordered or laminar state to irregular fluctuating or turbulent conditions. The distance x„ where this transition occurs, is characterised by the critical Reynolds number:

$$Re_C = \frac{u_\infty x_C}{\nu} = 3.2\cdot 10^5 \qquad (13)$$

Since the derived equations are only valid for laminar flow, the critical Reynolds number must not be exceeded in the simulations. The length of the plate was therefore chosen to 100mm, so that the Reynolds number is always smaller than Re_c.

Figure **4** shows the profiles of concentration and concentration force over the concentration boundary layer. The values are obtained for a particle diameter of 50nm at x = 50mm. However, the profiles are of similar shape at every other position along the plate, or for different particle dimensions.

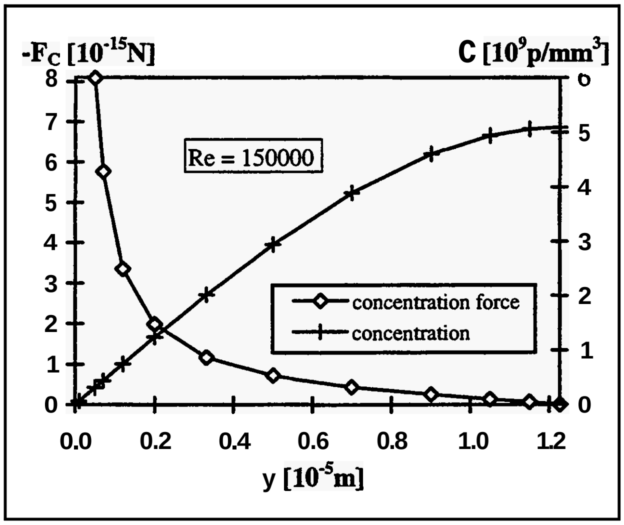

Figure 4 - Concentration profile and concentration force vs. distance along the plate

For y = δ_C = 0.12μm the concentration corresponds to the free-stream concentration C_∞; so the concentration gradient, and hence the concentration force, equals zero. Decreasing concentration closer to the plate leads to a drastic increase in the concentration force.

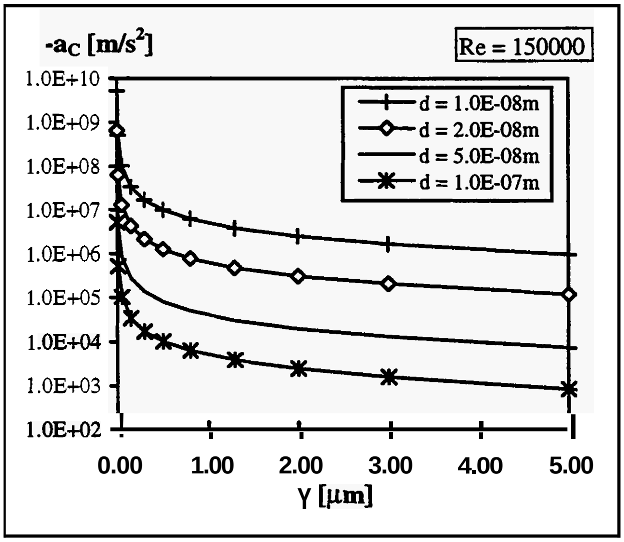

Figure 5 - Acceleration for various particle diameters

The influence of the size of the colloids on the concentration force was found to be minor. However, due to its strong influence on the particle mass, the diameter is of major importance for the particle acceleration a_C. The acceleration resulting from the influence of the concentration force is shown for different particle diameters in Figure 5.

As expected the acceleration increases with decreasing particle size. Figure 5 also indicates that small changes in particle size lead to considerable changes in acceleration. Typical values for the colloid diameter lie in the range of 20 to 50nm. The magnitude of the acceleration due to concentration variations illustrates that gravitational acceleration is negligible. Simulations assessing the influence of gravity resulted in identical scaling rates.

For the simulation with PHOENICS, the solution domain, the grid, and the boundary conditions were chosen **as** sketched in Figure 6.

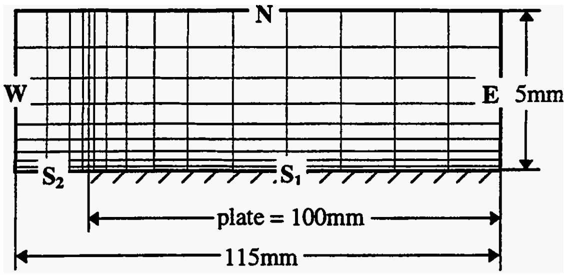

boundary conditions:
W (inlet): $p = \rho u_\infty$; $u = u_\infty$
N (outlet): $p = 0$
E (outlet): $p = 0$
S_1 (plate): $u = 0$
S_2: symmetry

grid dimensions:
115 cells in x-direction, fine mesh at leading edge of plate, Δx_{min} = 60 μm
21 cells in y-direction, fine mesh at plate surface, Δy_{min} = 24 μm

Figure 6 - The PHOENICS solution domain

The pressure is impressed on the velocity boundary layer by the outer flow. For the flat plate in parallel flow the pressure drop in the x-direction is zero. To minimise the solution domain, and therefore the computations, a constant pressure condition was provided at the northern boundary N. This boundary condition also allows fluid to leave the domain in order to take account of mass continuity. Velocities within the boundary layer obtained by simulation agreed very well with the exact solution of the Navier-Stokes equations. The high accuracy of the simulation was also confirmed by comparison of values for the frictional drag on the plate surface. Particles were injected at the western boundary W and withdrawn after deposition on the surface of the plate.

Figure 7 shows the simulated distribution of silica scaling on the plate surface. The particles depositing on the surface are counted individually per segment of 1mm length. The profiles reflect the silica deposition after approximately **1/500** second and therefore indicate an initial formation of silica scale. Figure 7 confirms that deposition rates increase with decreasing particle size. As mentioned earlier, diffusion processes at the leading edge of the plate are not entirely considered and therefore an average scaling rate over the first two mm is presented. The results of the simulation show that silica colloids mainly deposit at the front of the plate and deposition rates rapidly decrease with distance from the leading edge. For particle diameters of 10nm it was found that only particles released up to an entry height of 0.5µm above the plate deposit within the first 100mm. For particle diameters of 50nm this maximum entrance height is even smaller.

Figure 7 suggests an initial build-up of silica scale at the front of the plate. As a result, the shape of the laminar boundary layer changes and flow separation might occur. This also causes an earlier transition to turbulent flow and hence increases colloidal deposition.

6. CONCLUSIONS AND RECOMMENDATIONS

The equations in the present work are derived for the process of initial scaling of silica colloids on to a flat plate in laminar parallel flow. Originally, it was intended to take account of the build-up of silica scale by blocking off computational cells. However, the mechanisms leading to deposition of colloids were found to be restricted to a very small region close to the plate. In order to simulate the gradual development of the scale the grid would have to be extremely fine near the surface. At the same time the solution domain has to be large enough to enable an accurate representation of the fluid flow. Satisfying both conditions leads to a large number of grid cells and hence to large computing times. Problems occurred during the tracking of particles by GENTRA across very small cells. This phenomenon is currently being investigated by the programmers of PHOENICS. Resolving these problems would allow the process of silica deposition as a function of time to be investigated. Comparison with experimental results would reveal the accuracy of the simulations. In order to extend the model, further research requires the introduction of turbulence models and the representation of deposition mechanisms for turbulent fluid flow. Currently no general restrictions toward the generation of a model for the numerical simulation of the .process of silica scaling is known. Such a model would enable the modelling of scaling for any flow arrangement.

7. ACKNOWLEDGMENTS

We thank the Institute of Geological and Nuclear Sciences and Contact Energy Ltd. for their support.

8. REFERENCES

Crowe, C.T., Sharma, M.P. and Stock, D.E. (1977). ***The Particle-Source-In-Cell Model for Gas-Droplet Flows.*** ASME J. Fluids Eng., pp. 325-332.

Cussler, E.L. (1984). ***Diffusion, Mass Transfer in Fluid Systems.*** Cambridge University Press, New York.

Schlichting, H. (1979). ***Boundary-Layer Theory.*** McGraw-Hill, Inc., New York.

van de Ven, T.G.M. (1989). ***Colloidal Hydrodynamics.*** Academic Press, London.

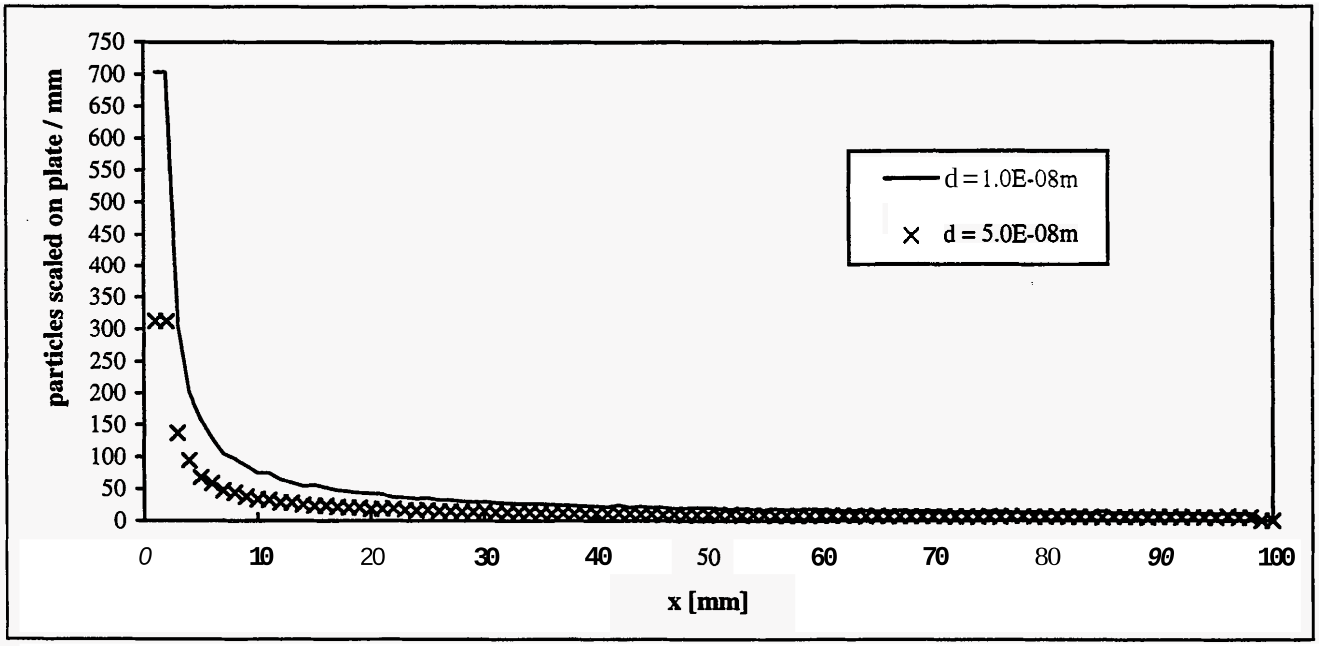

Figure 7 - Deposition of silica colloids on the plate surface